IEEE Photonics Journal
An IEEE Photonics Society Publication

Open Access

Azimuthal Turing Patterns, Bright and Dark Cavity Solitons in Kerr Combs Generated With Whispering-Gallery-Mode Resonators

Volume 5, Number 4, August 2013

Aurélien Coillet
Irina Balakireva
Rémi Henriet
Khaldoun Saleh
Laurent Larger, Senior Member, IEEE
John M. Dudley, Fellow, IEEE
Curtis R. Menyuk, Fellow, IEEE
Yanne K. Chembo, Senior Member, IEEE

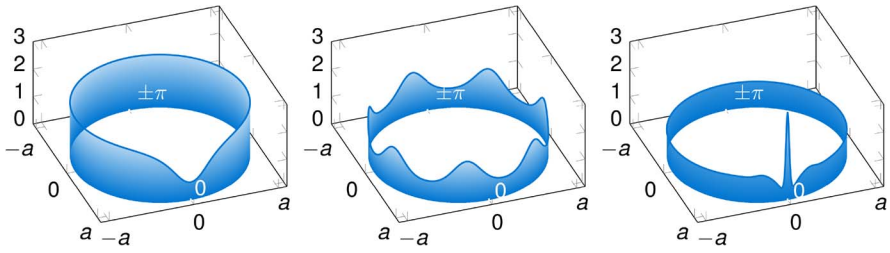

DOI: 10.1109/JPHOT.2013.2277882
1943-0655 © 2013 IEEE

Azimuthal Turing Patterns, Bright and Dark Cavity Solitons in Kerr Combs Generated With Whispering-Gallery-Mode Resonators

Aurélien Coillet,[1] Irina Balakireva,[1] Rémi Henriet,[1] Khaldoun Saleh,[1] Laurent Larger,[1] *Senior Member, IEEE*, John M. Dudley,[1] *Fellow, IEEE*, Curtis R. Menyuk,[2] *Fellow, IEEE*, and Yanne K. Chembo,[1] *Senior Member, IEEE*

[1]Department of Optics, FEMTO-ST Institute (CNRS UMR6174), 25030 Besançon, France
[2]Department of Computer Science and Electrical Engineering, The University of Maryland, Baltimore County, Baltimore, MD 21250 USA

DOI: 10.1109/JPHOT.2013.2277882

Manuscript received July 31, 2013; accepted August 2, 2013. Date of publication August 8, 2013; date of current version August 23, 2013. This work was supported by the European Research Council through Project NextPhase ERC StG 278616. Corresponding author: Y. K. Chembo (e-mail: yanne.chembo@femto-st.fr).

Abstract: We investigate the formation of cavity solitons in crystalline whispering-gallery-mode disk resonators that are pumped in different dispersion regimes. In the Fourier domain, these dissipative structures correspond to specific types of mode-locked Kerr optical frequency combs. Depending on the sign of the second-order chromatic dispersion and on the pumping conditions, we show that either bright or dark cavity solitons can emerge, and we show that these two regimes are associated with characteristic spectral signatures that can be discriminated experimentally. We use the Lugiato–Lefever spatiotemporal formalism to investigate the temporal dynamics leading to the formation of these azimuthal solitons, as well as the emergence of Turing patterns. The theoretical results are in excellent agreement with experimental measurements that are obtained using calcium and magnesium fluoride disk resonators pumped near 1550 nm.

Index Terms: Kerr optical frequency combs, solitons, Turing patterns, whispering gallery modes.

1. Introduction

Kerr optical frequency combs are sets of equidistant spectral lines in the optical domain, which are obtained through pumping a whispering gallery mode (WGM) resonator with a continuous wave (CW) laser [1]. The physical phenomenon behind Kerr comb generation is four-wave mixing, where two input photons α and μ may be converted into two output photons β and η following $\hbar\omega_\alpha + \hbar\omega_\mu \rightarrow \hbar\omega_\beta + \hbar\omega_\eta$, as long as they fulfill the requirements of energy and momentum conservation. Under optimal conditions, the photons originating from the pump laser are first transferred via this four-wave mixing to the neighboring cavity modes, and each excited mode is later on mixed with the others following the same mechanism. This cascaded process ultimately leads to the excitation of a broadband comb containing as much as several hundreds modes. If these spectral components remain phase-correlated, the corresponding time-domain optical signal is a train of equidistant, narrow, and ultra-low-jitter pulses yielding ultra-stable GHz or THz oscillations after photo-detection. These Kerr combs are promising alternatives to ultra-fast mode-locked lasers for several applications

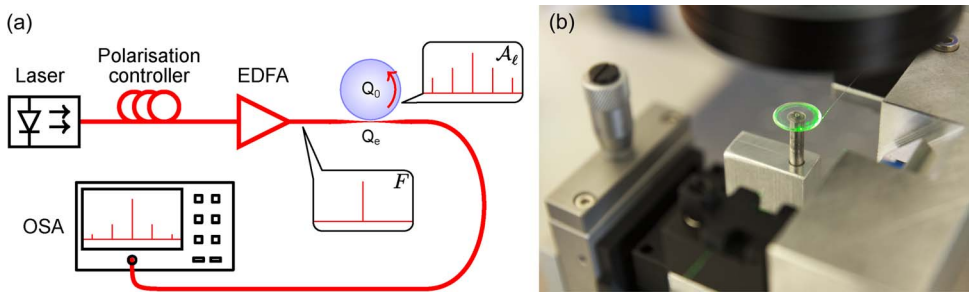

Fig. 1. (a) Experimental setup for the generation of Kerr combs in WGM resonators. The amplified CW laser pump at 1552 nm is coupled to the crystalline disk resonator using a tapered fiber, and the output is detected on an optical spectrum analyzer (OSA). (b) Photograph of the coupled resonator: the input signal goes from the fiber to the resonator through the evanescent field of the tapered fiber. Green laser light is here used for illustration purpose only.

in aerospace and communication engineering, as well as for sensing, time-frequency metrology or fundamental physics [2]–[7].

Kerr comb generation can be theoretically described by either a modal expansion or a spatiotemporal formalism. In the first case, a set of coupled ordinary differential equations tracks the individual dynamics of the complex envelope for each eigenmode of interest [8]–[10]. In the second case, a partial differential equation synthetically describes the dynamics of the overall intracavity field, which is the sum of the modal fields [11]–[14]. In the limit where the spectral extension of the comb is not octave spanning, it has been demonstrated in [13] that the spatiotemporal equation is mathematically equivalent to the Lugiato-Lefever equation (LLE) [15], which is a nonlinear Schrödinger equation (NLSE) with driving, damping and detuning. It is noteworthy that the LLE is a paradigmatic equation for dissipative cavity solitons, which are in our case pulse-like solutions in the time domain. Since narrow pulse formation is the key mechanism leading to broadband Kerr combs in the frequency domain (see for example [16]), it is necessary to understand this phenomenology in order to optimize the properties of the comb with regards to the targeted applications.

In this article, we investigate the formation of cavity solitons in WGM resonators. We here refer to these solitons as "azimuthal" because they are defined on a compact background with periodic boundary conditions. We particularly focus on the influence of the group velocity dispersion (GVD) on the formation of these solitons, and we show that depending on the initial conditions, bright solitons can be generated in the regime of anomalous GVD, while dark solitons can emerge in the regime of normal GVD. We also present the experimental Kerr optical frequency combs that correspond to the spectral signature of these localized dissipative structures.

The organization of the paper is the following. In the next section, we present the experimental system used to generate the Kerr combs. Then, the theoretical model is presented in Section 3. We discuss the case of Turing patterns and modulational instability in Section 4 when the GVD is anomalous. We also perform a numerical and experimental study, which enables us to understand the transient dynamics leading to the formation of these localized dissipative structures. Then, Sections 5 and 6 are devoted to the study of the formation of bright and dark cavity solitons, which arise in the anomalous and normal GVD regimes, respectively. The last section summarizes our results and concludes the article.

2. Experimental Setup

Our experimental setup is presented in Fig. 1. The WGM resonators used in our experiments are mm-size crystalline disks with a free spectral range (FSR) of the order of 5 GHz. The crystals are either calcium or magnesium fluoride (CaF_2 or MgF_2, respectively), and we polish the disks in order to obtain intrinsic quality factors of the order of 10^9 at 1550 nm. The resonators are pumped with a narrow linewidth CW semiconductor laser (RIO Orion, 1552 nm), amplified by a standard erbium-doped fiber amplifier (EDFA). The output power thereby reaches power levels as high as few hundreds of mW. This pump signal is then coupled into the crystalline WGM disk resonator via the evanescent field of a

tapered fiber whose diameter is as low as one micron. The intra-cavity field is coupled out through the same tapered fiber, and sent to the detection equipments. The output signal is first monitored using a slow photodiode in order to select a specific resonance and control the detuning between this resonance and the laser's wavelength. Then, a high resolution optical spectrum analyzer (APEX 2440B) is used to monitor the spectral characteristics of the output optical signal. In the next sections, the MgF_2 and CaF_2 will be used to investigate the anomalous and normal dispersion regimes, respectively.

3. Theoretical Modeling

Whispering gallery modes are characterized by two main properties, namely their eigenfrequency distribution and their modal linewidths.

On the first hand, the eigenmodes of the fundamental family are unambiguously determined by a single (azimuthal) eigennumber ℓ, which stands for the number of total internal reflections performed by a photon trapped within that mode. If we restrict ourselves to the case where only second-order dispersion is relevant, then the eigenfrequencies ω_ℓ of the resonator can be expanded around the eigenfrequency ω_{ℓ_0} of the pumped mode following $\omega_\ell = \omega_{\ell_0} + \zeta_1(\ell - \ell_0) + (\zeta_2/2)(\ell - \ell_0)^2$, where $\zeta_1 = c/an_0$ is the intermodal angular frequency (or free spectral range, FSR), a is the main radius of the disk, and n_0 is its refraction index at the frequency ω_{ℓ_0}. Note that for typical mm-size disks, we have $\zeta_1/2\pi \sim 10$ GHz. As a consequence, we have $\ell_0 \simeq \omega_{\ell_0}/\zeta_1 \sim 10^4$, and the round trip-time inside the cavity is given by $T = 2\pi/\zeta_1 \sim 100$ ps. The parameter ζ_2 stands for the second-order dispersion which measures the unequidistance of the eigenfrequencies at the lowest order. Typical values for crystalline resonators pumped near 1550 nm are such that $|\zeta_2|/2\pi \sim 1$ kHz, with ζ_2 being positive (negative) in the anomalous (normal) GVD regime. On the other hand, the modal linewidths $\Delta\omega_\ell$ depend on the frequency ω_ℓ and on the loss factor at that frequency. They are a measure of the energy storage capacity of the resonator since they are inversely proportional to the lifetimes for photons of frequency ω_ℓ inside the cavity.

In this study, we focus on combs whose spectral extension is far below octave spanning. In this case, the modes of interest are spectrally close to the pumped mode ℓ_0, so that their modal linewidths and spatial profiles can be considered as quasi-degenerated. It was shown in ref. [9] that in that case, the complex-valued slowly-varying envelopes $\mathcal{A}_\ell(t)$ of the modal fields obey the following system of coupled equations:

$$\frac{d\mathcal{A}_\ell}{dt} = -\frac{1}{2}\Delta\omega_{\text{tot}}\mathcal{A}_\ell + \delta(\ell - \ell_0)\frac{1}{2}\Delta\omega_{\text{tot}}\mathcal{F}_0 e^{i\sigma t} - ig_0 \sum_{\ell_m,\ell_n,\ell_p} \delta(\ell_m - \ell_n + \ell_p - \ell)\mathcal{A}_{\ell_m}\mathcal{A}^*_{\ell_n}\mathcal{A}_{\ell_p} e^{\left[i(\omega_{\ell_m} - \omega_{\ell_n} + \omega_{\ell_p} - \omega_\ell)t\right]}, \quad (1)$$

with $\delta(x)$ being the usual Kronecker function equal to 1 when $x = 0$ and to 0 otherwise. In this description, $\mathcal{A}_\ell$ stands for the intra-cavity amplitude of the ℓ-th mode, and it has been normalized such that $|\mathcal{A}_\ell|^2$ is the number of photons in the mode. The first term in the right-hand side (RHS) stands for the intrinsic and extrinsic (or coupling) losses: it is characterized by the total linewidth $\Delta\omega_{\text{tot}} = \Delta\omega_{\text{in}} + \Delta\omega_{\text{ext}}$, where $\Delta\omega_{\text{in,ext,tot}} = \omega_{\ell_0}/Q_{\text{in,ext,tot}}$. The parameters Q_{in}, Q_{ext}, Q_{tot} are respectively the intrinsic, extrinsic and total (or loaded) quality factors while the corresponding linewidths are analogously defined. The second term in the RHS of Eq. (1) corresponds to the laser pump. The parameter $\sigma = \Omega_0 - \omega_{\ell_0}$ is the detuning of the angular laser frequency Ω_0 with respect to the modal resonance. Efficient pumping generally requires $|\sigma|$ to be smaller than the modal linewidth $\Delta\omega_{\text{tot}}$. Using the theory for mode coupling in resonators [17], it can be shown that the intensity of this external pumping term is such that $(1/2)\Delta\omega_{\text{tot}}\mathcal{F}_0 = \sqrt{\Delta\omega_{\text{ext}}}\sqrt{P/\hbar\Omega_0}$, where P is the intensity (in W) of the laser pump at the input of the resonator [18]. The optical phase reference is set by this pump radiation, so that we may choose $\mathcal{F}_0$ to be real-valued and positive. The last term in the RHS of Eq. (1) stands for the four-wave mixing interaction. The nonlinear gain parameter $g_0 = (n_2 c\hbar\omega^2_{\ell_0}/n_0^2 V_0)$ where $\hbar$ is Planck's constant, n_2 is the Kerr coefficient at the frequency Ω_0, and V_0 is the effective mode volume of the pumped mode. The Kronecker function imposes that interacting photons fulfill the momentum conservation requirement $\ell_m + \ell_p = \ell_n + \ell$. The term $\omega_{\ell_m} - \omega_{\ell_n} + \omega_{\ell_p} - \omega_\ell$ in the exponential argument

within the summation stands for the phase detuning induced by the second-order dispersion, since it vanishes when ζ_2 is set to zero according to Taylor expansion of the eigenfrequencies ω_ℓ.

It has recently been shown in ref. [13] that the modal approach represented in Eqs. (1) has an *exact* spatiotemporal counterpart, which is a normalized Lugiato-Lefever equation with periodic boundary conditions:

$$\frac{\partial \psi}{\partial \tau} = -(1 + i\alpha)\psi + i|\psi|^2\psi - i\frac{\beta}{2}\frac{\partial^2 \psi}{\partial \theta^2} + F, \tag{2}$$

where the main variable is the total intracavity field ψ. This field is linked to the modal fields $\mathcal{A}_\ell$ through

$$\psi(\theta, \tau) = \sqrt{\frac{2g_0}{\Delta\omega_{\text{tot}}}} \sum_\ell \mathcal{A}_\ell^*(\tau) e^{\left[i(\ell-\ell_0)\theta + i\frac{1}{2}\beta(\ell-\ell_0)^2\tau\right]}, \tag{3}$$

and it is important to note here that ψ is a moving frame variable, in the sense that the group-velocity motion has been removed in Eq. (2). The arguments of ψ are $\theta \in [-\pi, \pi]$ which is the azimuthal angle along the rim of the disk, and $\tau = t/2\tau_{\text{ph}}$ which is the dimensionless time, with $\tau_{\text{ph}} = 1/\Delta\omega_{\text{tot}}$ being the photon lifetime in the coupled cavity. The dimensionless parameters of this normalized LLE are the frequency detuning $\alpha = -2\sigma/\Delta\omega_{\text{tot}}$, the dispersion parameter $\beta = -2\zeta_2/\Delta\omega_{\text{tot}}$, and the pump term

$$F = \sqrt{\frac{2g_0}{\Delta\omega_{\text{tot}}}}\mathcal{F}_0^* = \sqrt{\frac{8g_0\Delta\omega_{\text{ext}}}{\Delta\omega_{\text{tot}}^3}\frac{P}{\hbar\Omega_0}}. \tag{4}$$

In terms of order of magnitude, we typically have $|\psi|^2 \sim 1$, $|\alpha| \sim 1$ (can vary linearly from ~ -3 to 3), $|\beta| \ll 1$, and $F \sim 1$. We will use this spatiotemporal formalism to investigate the time-domain dynamics leading to pulse formation in both the anomalous ($\beta < 0$) and normal ($\beta > 0$) GVD regimes. The numerical simulations have been performed using the Split-step Fourier method, with a time-step of 1 ns, and the computation time was about 5 min to compute the dynamics of the system for 1 ms. It should be noted that while our theoretical modeling focuses on the field inside the cavity, the experiments can only give the intensity at the output of the fiber taper. These two quantities are linked by $S_{\text{out}}(t) = -F + \sqrt{\Delta\omega_{\text{ext}}}\psi(0, t)$ according to the theory of coupled resonators [17], where $|S_{\text{out}}|^2$ is the dimensionless output power. As a consequence, the pump field F adds to a portion of the intracavity field ψ at the detector, which has to be taken into account when comparing the experimental and computational spectra.

4. Turing Rolls via Modulational Instability in the Anomalous GVD Regime

The conditions under which Kerr comb generation occurs have been the focus of numerous studies, and the underlying theory is far from being complete. In most cases, Kerr combs are generated through modulational instability (MI) in the regime of anomalous GVD. In this context, a flat background is destabilized by weak perturbations leading to the formation of short pulses. In optics, this phenomenology is generally observed in optical fiber systems [19], and is a widely studied topic of research. Such MI-induced combs had been observed experimentally, and the threshold behavior leading to their apparition has been investigated in detail in ref. [9] using the modal expansion approach. It had been demonstrated that these patterns, which corresponds to the so-called *primary combs* [9], arise after a pitchfork bifurcation when the intracavity field reaches the threshold value $|\psi|_{\text{th}}^2 = 1$. The pattern is characterized by multiple rolls traveling circumferentially inside the cavity, and near threshold, their number can be analytically determined as the closest integer value to

$$l_{\text{th}} = \sqrt{\frac{2}{\zeta_2}[\sigma + \Delta\omega_{\text{tot}}]} = \sqrt{\frac{4}{\beta}\left[\frac{\alpha}{2} - 1\right]} \tag{5}$$

for $\alpha < 2$ (see ref. [9]).

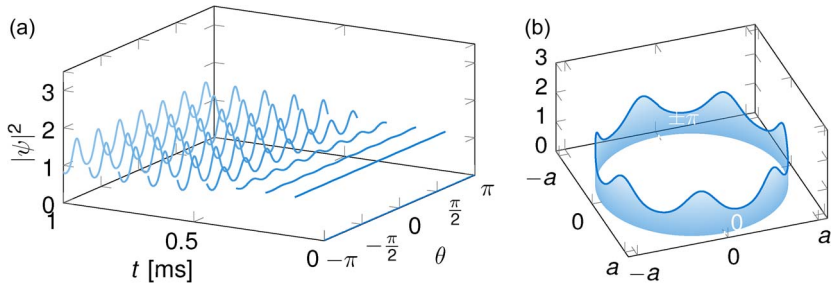

Fig. 2. Numerical simulation of the generation of Turing rolls via MI. The parameters are $\alpha = -0.5$, $\beta = -0.1$ and $F = 1.89$, and they lead to the formation of 7 rolls. (a) Formation of the rolls from a noisy, quasi-flat initial condition. (b) 3D visualization of the Turing pattern in the WGM cavity. This pattern is fixed in the moving frame, but it rotates in the laboratory frame with an angular frequency $\zeta_1 = c/an_0$. This is also the case for Figs. 4(b) and 6(b).

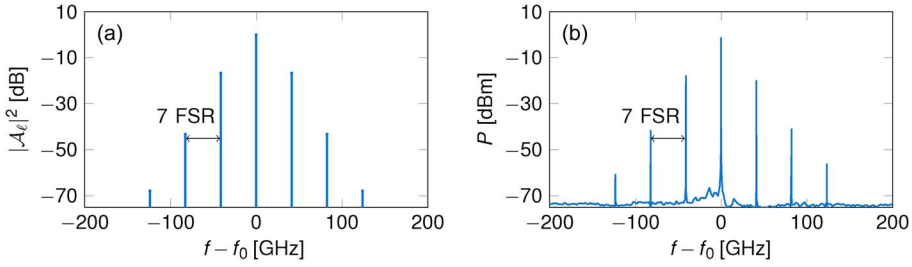

Fig. 3. (a) Numerical spectrum of the Kerr comb induced by the Turing pattern of Fig. 2. (b) Experimental Kerr comb spectrum obtained with a MgF_2 resonator, in the anomalous dispersion regime. In multiple-FSR combs, the multiplicity l_{th} in the spectral domain is equal to the number of rolls in the azimuthal direction.

Fig. 2 shows how these rolls are formed in the WGM cavity. The corresponding numerical spectrum is displayed in Fig. 3(a) and it can be seen that they are characterized by a multiple-FSR spacing between the spectral components, the multiplicity being equal to the number of rolls. We have experimentally observed these patterns in our system, consisting of a magnesium fluoride WGM disk-resonator with refraction index $n_0 = 1.37$ and radius $a = 5.66$ mm, yielding a FSR $\zeta_1/2\pi = 5.9$ GHz. The intrinsic quality factor of the disk was equal to 1.7×10^9, and the overall dispersion of the resonator was anomalous at the pump wavelength ($\zeta_2/2\pi \sim 1$ kHz). The experimental spectra is presented in Fig. 3(b), and it can be seen that satisfying agreement is achieved with the theoretical spectrum. At the experimental level, this spectrum appeared to be relatively insensitive to external perturbations, indicating that these patterns are particularly robust.

In the context of dissipative cavity structures, these patterns are sometimes referred to as *Turing patterns*, in reference to Turing's seminal work on morphogenesis [20], where he theoretically predicted the spontaneous breakdown of symmetry and homogeneity through the emergence of dissipative patterns in reaction-diffusion systems. It is a striking coincidence that Turing's toy-model was a "*continuous ring of tissue*", and one of his main findings was that "*in the most interesting form stationary waves appear on the ring*" [Turing rolls of Fig. 2(b)].

As far as the LLE with anomalous dispersion is concerned, it is worth noting that the super- or sub-critical nature of Turing patterns have been studied in detail in refs. [21]–[23], and it is known that they arise for $\alpha < 41/30$ and $\alpha > 41/30$, respectively. The soft (supercritical) and hard (subcritical) excitation regimes for Kerr combs have also been numerically investigated in ref. [24] using a modal expansion approach. We show in the next sections that beside these MI-induced combs, it is possible to observe cavity solitons, which are characterized by intrinsically different spectra.

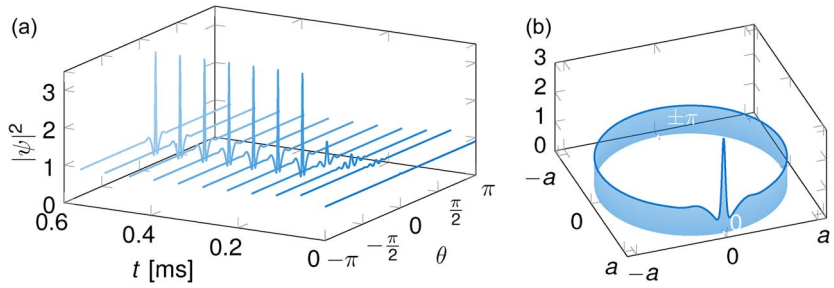

Fig. 4. Numerical simulation of the generation of a bright azimuthal cavity soliton. The parameters are $\alpha = 1.7$, $\beta = -0.002$, and $F = 1.22$. (a) Formation of the bright soliton from a pulse-like initial condition. (b) 3D visualization of the bright cavity soliton in the WGM cavity.

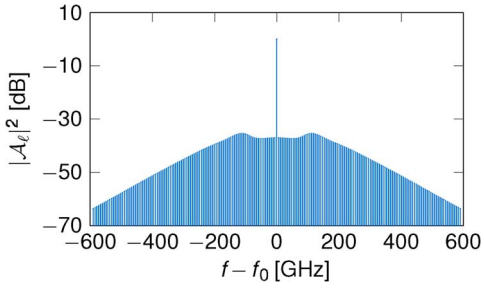

Fig. 5. Numerical spectrum of the Kerr comb induced by the bright cavity soliton of Fig. 4. This comb has a single-FSR spacing.

5. Bright Azimuthal Cavity Solitons in the Anomalous GVD Regime

Previous research had proven the possibility of cavity solitons in systems described by the LLE. A noteworthy example can be found in refs. [25], [26] where 2D bright cavity solitons were theoretically evidenced in Kerr media illuminated by a free-propagating laser beam. That system was physically similar to the one originally considered by Lugiato and Lefever [15], where the second order derivative corresponded to a diffraction term, instead of a dispersive term as in our case.

Fig. 4 shows the emergence of this soliton when the flat background is initially excited by a pulse-like perturbation. The bright cavity soliton is a sub-critical localized dissipative structure, in the sense that it does not emerge for arbitrarily small perturbations of the background. The well known sech^2 soliton which is the fundamental solution of the NLSE maintains its shape by achieving a balance between nonlinearity and dispersion; cavity solitons have to achieve as well a balance between energy gain (from the laser pump) and loss (since the cavity is dissipative). Unlike the NLSE soliton, the LLE soliton stands on a non-zero background, and is generally characterized by a small pedestal oscillation. In our case, bright solitons are sub-critical localized dissipative structures, which are indirectly linked to sub-critical Turing patterns. That is why they can theoretically not be observed for $\alpha < 41/30$ (in general, they arise for $\alpha \sim 2$). They are therefore intrinsically different from the Turing rolls displayed in Fig. 2 since unlike solitons, these supercritical Turing rolls can be as small as one wants above threshold. Actually, just above threshold, the "rolls" are sinusoidal, and thereby induce only two modulation sidebands. The apparition of this 3-modes Kerr comb corresponds to the typical phenomenology of MI, and has been investigated in detail in ref. [9]. It is also noteworthy that Turing rolls are not localized structures because they inherently depend on the boundary conditions, since there is always an integer number of them along the rim. On the other hand, solitons are indeed localized structures, and they do not "see" the boundaries when they are far enough. The soliton of Fig. 4(a) typically behaves as if its background had an infinite extension.

The spectrum corresponding to this soliton is presented in Fig. 5. Since there is only one pulse traveling in the cavity, all the WGMs are excited and mode locked. Less than 10 modes where excited in the MI regime, but here it can be seen that more than 200 modes are excited. The cavity

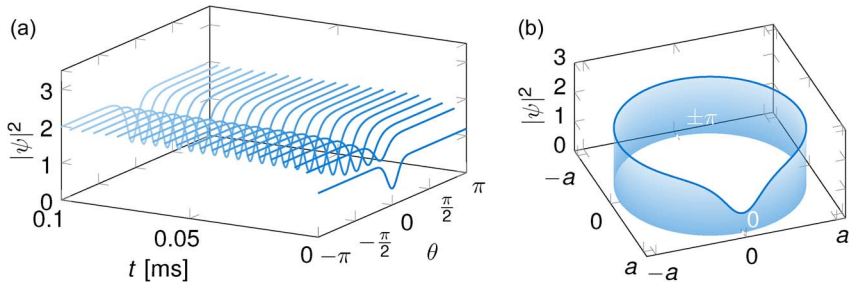

Fig. 6. Numerical simulation of the generation of a dark azimuthal cavity soliton. The parameters are $\alpha = 2.05$, $\beta = 0.0125$, and $F = 1.4$. (a) Formation of the dark soliton from a pulse-like initial condition. (b) 3D visualization of the dark cavity soliton in the WGM cavity.

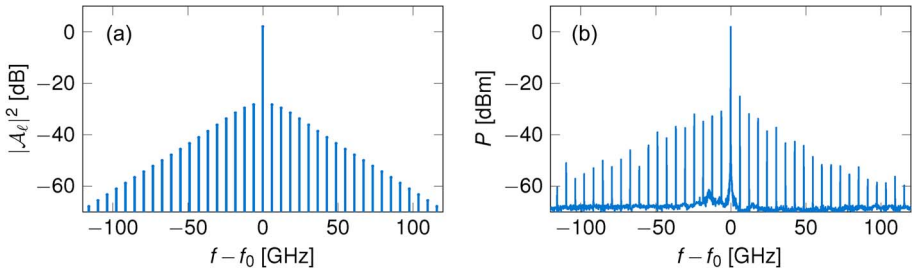

Fig. 7. (a) Numerical spectrum of the Kerr comb induced by the dark cavity soliton of Fig. 6. This comb has a single-FSR spacing. (b) Experimental Kerr comb spectrum of a dark soliton obtained in a CaF_2 resonator whose dispersion is normal at 1550 nm.

soliton power spectrum is very characteristic and can be unambiguously identified by its single-FSR line-spacing and its wing-like shape around the pump; this particular feature is in fact induced by the pedestal. A theoretical analysis of the formation of such solitons is proposed in refs. [13], [14], and a noteworthy reference were these solitons have been experimentally studied is ref. [16].

6. Dark Azimuthal Cavity Solitons in the Normal GVD Regime

It is known that the MI observed in the anomalous dispersion regime cannot arise in the normal GVD regime because the pump cannot be phase-matched with the small modulation-induced spectral sidebands. For this reason, it was thought for some time that stable Kerr comb could not exist in the normal GVD regime. However, some early works did provide scientific motivations for the possibility of MI in the normal GVD regime when strong (instead of weak) perturbations of the CW background are considered. For instance, using the NLSE formalism, it had been shown that MI can be induced in the normal GVD regime by two co-propagating optical fields interacting with each other through cross-phase modulation [27]. In fiber-ring cavities, which are similar in many ways to WGM disk resonators, MI may arise in the normal GVD regime owing to the extra degree of freedom provided by the frequency detuning between the pump laser and the resonant cavity [28]. In the specific context of WGM disk resonators, the modal expansion model predicted the possibility of Kerr comb generation for all but zero GVD [9]. Normal GVD Kerr combs have also been theoretically and experimentally studied in (CaF_2) WGM resonators [29]–[31].

In their review article [32], Kivshar and Luther-Davies define optical dark solitons as localized nonlinear waves (or "holes") existing on a stable continuous wave (or extended finite-width). We show here that these dark solitons can also be observed in our system. The numerical simulations of Fig. 6(a) shows how a dip-like perturbation of the background can lead to a dark cavity soliton. This soliton has been experimentally evidenced as well. The WGM resonator in this case is a calcium fluoride disk with refraction index $n_0 = 1.43$, radius $a = 5.5$ mm and intrinsic quality factor

equal to 0.7×10^9, yielding a FSR $\zeta_1/2\pi = 6.1$ GHz. The overall dispersion of the resonator is weakly normal for our pump wavelength, and is of the order of $\zeta_2/2\pi \sim -1$ kHz.

The theoretical spectrum of the dark soliton is displayed in Fig. 7(a) and it agrees very well with the experimental measurement. This spectrum is characterized by a single FSR spacing between the comb teeth, and the triangular-like decrease of the sidemode powers. However, it was experimentally noted that this dark soliton is not a very robust solution, as it decays to a flat background steady state when submitted to relatively modest external perturbations.

7. Conclusion

In conclusion, we have provided numerical and experimental evidence of bright and dark solitons in crystalline WGM disk resonators, and we have discussed the conditions leading to their emergence in the context of Kerr comb generation. The Lugiato-Lefever equation has enabled to analyze the dynamical properties of these solitons. It is important to study in more detail the importance of GVD in future works, with the objective of tailoring for the spectral properties of the comb [33], [34]. It will be interesting as well to investigate the stability of these solitons, and to explore the dynamical properties of the wide variety of Kerr combs that are experimentally observable [35].

Acknowledgment

The authors also acknowledge support from the *Centre National d'Etudes Spatiales* (CNES, France) through the Project SHYRO, from the ANR project ORA, from the *Région de Franche-Comté*, France, and from the Labex ACTION. Authors would also like to acknowledge for the support of the *Mésocentre de Calcul de Franche-Comté*.

References

[1] T. Kippenberg, R. Holzwarth, and S. Diddams, "Microresonator-based optical frequency combs," *Science*, vol. 332, no. 6029, pp. 555–559, Apr. 2011.
[2] F. Ferdous, H. Miao, D. E. Leaird, K. Srinivasan, J. Wang, L. Chen, L. T. Varghese, and A. M. Weiner, "Spectral line-by-line pulse shaping of on-chip microresonator frequency combs," *Nat. Photon.*, vol. 5, pp. 770–776, Oct. 2011.
[3] A. A. Savchenkov, A. B. Matsko, W. Liang, V. S. Ilchenko, D. Seidel, and L. Maleki, "Kerr combs with selectable central frequency," *Nat. Photon.*, vol. 5, no. 5, pp. 293–296, Apr. 2011.
[4] S. B. Papp and S. A. Diddams, "Spectral and temporal characterization of a fused-quartz-microresonator optical frequency comb," *Phys. Rev. A*, vol. 84, no. 5, pp. 053833-1–053833-7, Nov. 2011.
[5] P. Del'Haye, S. B. Papp, and S. A. Diddams, "Hybrid electro-optically modulated microcombs," *Phys. Rev. Lett.*, vol. 109, no. 26, pp. 263901-1–263901-5, Dec. 2012.
[6] T. Herr, K. Hartinger, J. Riemensberger, C. Y. Wang, E. Gavartin, R. Holzwarth, M. L. Gorodetsky, and T. J. Kippenberg, "Universal formation dynamics and noise of Kerr-frequency combs in microresonators," *Nat. Photon.*, vol. 6, no. 7, pp. 480–487, Jun. 2012.
[7] C. Y. Wang, T. Herr, P. Del'Haye, A. Schliesser, J. Hofer, R. Holzwarth, T. W. Hänsch, N. Picqué, and T. J. Kippenberg, "Mid-infrared optical frequency combs at 2.5 μm based on crystalline microresonators," *Nat. Commun.*, vol. 4, p. 1345, Jan. 2013.
[8] A. A. Savchenkov, A. B. Matsko, D. Strekalov, M. Mohageg, V. S. Ilchenko, and L. Maleki, "Low threshold optical oscillations in a whispering gallery mode CaF_2 resonator," *Phys. Rev. Lett.*, vol. 93, no. 24, pp. 243905-1–243905-4, Dec. 2004.
[9] Y. K. Chembo and N. Yu, "Modal expansion approach to optical-frequency-comb generation with monolithic whispering-gallery-mode resonators," *Phys. Rev. A*, vol. 82, no. 3, pp. 033801-1–033801-18, Sep. 2010.
[10] Y. K. Chembo, D. V. Strekalov, and N. Yu, "Spectrum and dynamics of optical frequency combs generated with monolithic whispering gallery mode resonators," *Phys. Rev. Lett.*, vol. 104, no. 10, pp. 103902-1–103902-4, Mar. 2010.
[11] I. H. Agha, Y. Okawachi, and A. L. Gaeta, "Theoretical and experimental investigation of broadband cascaded four-wave mixing in high-Q microspheres," *Opt. Exp.*, vol. 17, no. 18, pp. 16 209–16 215, Aug. 2009.
[12] A. B. Matsko, A. A. Savchenkov, W. Liang, V. S. Ilchenko, D. Seidel, and L. Maleki, "Mode-locked Kerr frequency combs," *Opt. Lett.*, vol. 36, no. 15, pp. 2845–2847, Aug. 2011.
[13] Y. K. Chembo and C. R. Menyuk, "Spatiotemporal Lugiato-Lefever formalism for Kerr-comb generation in whispering-gallery-mode resonators," *Phys. Rev. A*, vol. 87, no. 5, pp. 053852-1–053852-4, May 2013.
[14] S. Coen, H. G. Randle, T. Sylvestre, and M. Erkintalo, "Modeling of octave-spanning Kerr frequency combs using a generalized mean-field Lugiato-Lefever model," *Opt. Lett.*, vol. 38, no. 1, pp. 37–39, Jan. 2013.
[15] L. A. Lugiato and R. Lefever, "Spatial dissipative structures in passive optical systems," *Phys. Rev. Lett.*, vol. 58, no. 21, pp. 2209–2211, May 1987.
[16] T. Herr, V. Brasch, J. D. Jost, C. Y. Wang, N. M. Kondratiev, M. L. Gorodetsky, and T. J. Kippenberg, "Mode-locking in an optical microresonator via soliton formation," 2012, arXiv:1211.0733.

[17] H. A. Haus, *Waves and Fields in Optoelectronics*. Englewood Cliffs, NJ, USA: Prentice-Hall, 1984.
[18] A. Coillet, R. Henriet, P. Salzenstein, K. Phan Huy, L. Larger, and Y. K. Chembo, "Time-domain dynamics and stability analysis of optoelectronic oscillators based on whispering-gallery mode resonators," *IEEE J. Sel. Top. Quantum Electron.*, vol. 19, no. 5, p. 6000112, May 2013.
[19] K. Tai, A. Hasegawa, and A. Tomita, "Observation of modulational instability in optical fibers," *Phys. Rev. Lett.*, vol. 56, no. 2, pp. 135–138, Jan. 1986.
[20] A. M. Turing, "The chemical basis of morphogenesis," *Phil. Trans. of the R. Soc. Ser. B*, vol. 237, no. 641, pp. 37–72, Aug. 1952.
[21] A. J. Scroggie, W. J. Firth, G. S. McDonald, M. Tlidi, R. Lefever, and L. A. Lugiato, "Pattern formation in a passive Kerr cavity," *Chaos Solitons Fractals*, vol. 4, no. 8/9, pp. 1323–1354, Aug./Sep. 1994.
[22] T. Miyaji, I. Ohnishi, and Y. Tsutsumi, "Bifurcation analysis to the Lugiato-Lefever equation in one space dimension," *Physica D*, vol. 239, no. 23/24, pp. 2066–2083, Nov. 2010.
[23] G. Kozyreff, "Localized Turing patterns in nonlinear optical cavities," *Physica D*, vol. 241, no. 10, pp. 939–946, May 2012.
[24] A. B. Matsko, A. A. Savchenkov, V. S. Ilchenko, D. Seidel, and L. Maleki, "Hard and soft excitation regimes of Kerr frequency combs," *Phys. Rev. A*, vol. 85, no. 2, pp. 023830-1–023830-5, Feb. 2012.
[25] W. J. Firth, G. K. Harkness, A. Lord, J. M. McSloy, D. Gomila, and P. Colet, "Dynamical properties of two-dimensional Kerr cavity solitons," *J. Opt. Soc. Am. B*, vol. 19, no. 4, pp. 747–752, Apr. 2002.
[26] D. Gomila, M. A. Matías, and P. Colet, "Excitability mediated by localized structures in a dissipative nonlinear optical cavity," *Phys. Rev. Lett.*, vol. 94, no. 6, pp. 063905-1–063905-4, Feb. 2005.
[27] G. P. Agrawal, "Modulation instability induced by cross-phase modulation," *Phys. Rev. Lett.*, vol. 59, no. 8, pp. 880–883, Aug. 1987.
[28] M. Haelterman, S. Trillo, and S. Wabnitz, "Additive-modulation-instability ring laser in the normal dispersion regime of a fiber," *Opt. Lett.*, vol. 17, no. 10, pp. 745–747, May 1992.
[29] A. A. Savchenkov, E. Rubiola, A. B. Matsko, V. S. Ilchenko, and L. Maleki, "Phase noise of whispering gallery photonic hyper-parametric microwave oscillators," *Opt. Exp.*, vol. 16, no. 6, pp. 4130–4144, Mar. 2008.
[30] A. A. Savchenkov, A. B. Matsko, V. S. Ilchenko, I. Solomatine, D. Seidel, and L. Maleki, "Tunable optical frequency comb with a crystalline whispering gallery mode resonator," *Phys. Rev. Lett.*, vol. 101, no. 9, pp. 093902-1–093902-4, Aug. 2008.
[31] A. B. Matsko, A. A. Savchenkov, and L. Maleki, "Normal group-velocity dispersion Kerr frequency comb," *Opt. Lett.*, vol. 37, no. 1, pp. 43–45, Jan. 2012.
[32] B. Luther-Davies and Y. S. Kivshar, "Dark optical solitons: Physics and applications," *Phys. Reports*, vol. 298, no. 2/3, pp. 81–197, May 1998.
[33] I. S. Grudinin, L. Baumgartel, and N. Yu, "Frequency comb from a microresonator with engineered spectrum," *Opt. Exp.*, vol. 20, no. 6, pp. 6604–6609, Mar. 2012.
[34] M. R. E. Lamont, Y. Okawachi, and A. L. Gaeta, "Route to stabilized ultrabroadband microresonator-based frequency combs," May 2013, arXiv:1305.4921.
[35] F. Leo, L. Gelens, P. Emplit, M. Haelterman, and S. Coen, "Dynamics of one-dimensional Kerr cavity solitons," *Opt. Exp.*, vol. 21, no. 7, pp. 9180–9191, Apr. 2013.